BMC Cancer

RESEARCH Open Access

Comprehensive pan-cancer analysis reveals EPHB2 is a novel predictive biomarker for prognosis and immunotherapy response

Shengshan Xu[1*], Youbin Zheng[2], Min Ye[1], Tao Shen[1], Dongxi Zhang[1], Zumei Li[1] and Zhuming Lu[1*]

Abstract

Purpose Recent studies have increasingly linked Ephrin receptor B2 (EPHB2) to cancer progression. However, comprehensive investigations into the immunological roles and prognostic significance of EPHB2 across various cancers remain lacking.

Methods We employed various databases and bioinformatics tools to investigate the impact of EPHB2 on prognosis, immune infiltration, genome instability, and response to immunotherapy. Validation of the correlation between EPHB2 expression and M2 macrophages included analyses using bulk and single-cell transcriptomic datasets, spatial transcriptomics, and multi-fluorescence staining. Moreover, we performed cMap web tool to screen for EPHB2-targeted compounds and assessed their potential through molecular docking and dynamics simulations. Additionally, in vitro validation using lung adenocarcinoma (LUAD) cell lines was conducted to confirm the bioinformatics predictions about EPHB2.

Results EPHB2 dysregulation was observed across multiple cancer types, where it demonstrated significant diagnostic and prognostic value. Gene Set Enrichment Analysis (GSEA) indicated that EPHB2 is involved in enhancing cellular proliferation, invasiveness of cancer cells, and modulation of the anti-cancer immune response. Furthermore, it is emerged as a pan-cancer marker for M2 macrophage infiltration, supported by integrated analyses of transcriptomics and multiple fluorescence staining. In LUAD cells, knockdown of EPHB2 expression led to a decrease in both cell proliferation and migratory activity.

Conclusion EPHB2 expression may serve as a pivotal indicator of M2 macrophage infiltration, offering vital insights into tumor dynamics and progression across various cancers, including lung adenocarcinoma, highlighting its significant prognostic and therapeutic potential for further exploration.

Keywords Pan-cancer analysis, M2 macrophage, Biomarker, Prognosis, Immunotherapy

*Correspondence:
Shengshan Xu
xushengshan@jmszxyy.com.cn
Zhuming Lu
lzm219@jnu.edu.cn
[1]Department of Thoracic Surgery, Jiangmen Central Hospital, Jiangmen, Guangdong, China
[2]Department of Radiology, Jiangmen Wuyi Hospital of Traditional Chinese Medicine, Jiangmen, Guangdong, China

Introduction

Cancer significantly impacts global mortality and public health. According to data from the Global Cancer Research Center for the year 2020, there were approximately 19.3 million new cancer cases and almost 10 million deaths attributed to cancer [1]. Despite advancements in surgical techniques and early detection have reduced mortality rates, the heterogeneous nature of tumors and their propensity to relapse and spread continue to result in generally low survival rates for many cancers [2]. The integration of prognostic biomarkers from research into clinical practice remains sluggish, despite the growing adoption of personalized cancer therapies [3]. Immunotherapy, particularly immune checkpoint inhibitors, has become a pivotal component of cancer treatment, demonstrating the potential for long-term remission and offering prospects for lasting cures [4]. This underscores the importance of identifying immune-related biomarkers for broader clinical application.

Eph receptors, the largest group of receptor tyrosine kinases, play crucial roles in developmental processes and cellular balance, such as cell adhesion, migration, and axon guidance [5–7]. Specifically, Ephrin receptor B2 (EPHB2) has been implicated in promoting invasion in glioblastoma multiforme (GBM)via paxillin phosphorylation [8], and is linked to enhanced proliferation, invasion, and metastasis in various cancers, including cutaneous squamous cell carcinoma [9], cholangiocarcinoma [10], cervical cancer [11], lung adenocarcinoma [12], gastric cancer [13], and medulloblastoma [14]. Conversely, reduced EPHB2 expression has been linked with poorer outcomes in colorectal cancer [15], illustrating its diverse regulatory roles in cancer progression and potential impact on the tumor immune microenvironment. Despite these associations, there is a notable gap in pan-cancer studies exploring EPHB2's comprehensive predictive value for prognosis and immunotherapy responsiveness. Focused research on individual cancer types may fail to capture the broader mechanistic insights of this gene across cancers, underscoring the need for systematic, pan-cancer investigations to fully understand EPHB2's multifaceted roles in oncology, which could drive future research and clinical strategies. In this study, we conducted a comprehensive pan-cancer analysis of EPHB2, employing multiple datasets spanning various cancers to elucidate the correlations between EPHB2 expression, clinical features, and multi-omic heterogeneity. This study particularly investigates EPHB2's potential role in modulating immune cell infiltration across cancers, with a focus on its status as a biomarker for M2 macrophage infiltration, validated via fluorescent staining. Furthermore, connectivity map analyses were conducted to identify potential compounds targeting EPHB2's oncogenic effects, complemented by in vitro experiments in lung adenocarcinoma cell lines to confirm its regulatory impact on cell proliferation. These efforts provide valuable insights that could inform the development of new cancer therapies and enhance our understanding of EPHB2 in cancer progression and therapy. An overview of the study's methodology is depicted in Fig. 1.

Materials and methods

Comprehensive Data gathering and Processing Across multiple cancers

We sourced pan-cancer data on EPHB2 expression and related clinical characteristics through the UCSC Xena platform, utilizing The Cancer Genome Atlas (TCGA, http://cancergenome.nih.gov/) and Genotype-Tissue Expression (GTEx, https://gtexportal.org/home/) databases [16]. Additionally, EPHB2 expression across pan-cancer cell lines was examined using the Cancer Cell Line Encyclopedia (CCLE, https://sites.broadinstitute.org/ccle) [17]. The single-nucleotide variation (SNV) data were sourced from the cBioPortal (http://cbioportal.org) for Cancer Genomics [18, 19]. Detailed information on the 33 tumor types analyzed is available in Supplementary Table 1.

Comparative analysis of EPHB2 expression across Pan-cancer

Initial analyses of EPHB2 mRNA expression were performed using data from TCGA and GTEx databases. Expression differences across cancer subtypes and stages were visualized using boxplots. Protein level comparisons between tumors and corresponding healthy tissues were conducted using Clinical Proteomic Tumor Analysis Consortium (CPTAC, https://portal.gdc.cancer.gov/) data [20].

Analysis of diagnostic and prognostic potential

Receiver Operating Characteristic (ROC) curves were generated using the "pROC" R package and Kaplan-Meier survival analyses were conducted with the the "survminer" R package [21]. Optimal cut-off scores were used to evaluate overall survival (OS), disease-specific survival (DSS), progression-free interval (PFI), and disease-free interval (DFI) in cohorts, maintaining a minimum high-to-low expression ratio of 0.3. The "survfit" function facilitated the log-rank tests, and univariate Cox regression analyses were performed to assess EPHB2's prognostic relevance using the "survival" and "forestplot" packages in R.

Genomic alteration and mutational burden analyses

Mutation types and distributions of EPHB2 were analyzed using the COSMIC database (https://cancer.sanger.ac.uk/cosmic/) [22] and cBioPortal. Spearman's correlation analysis examined associations between EPHB2

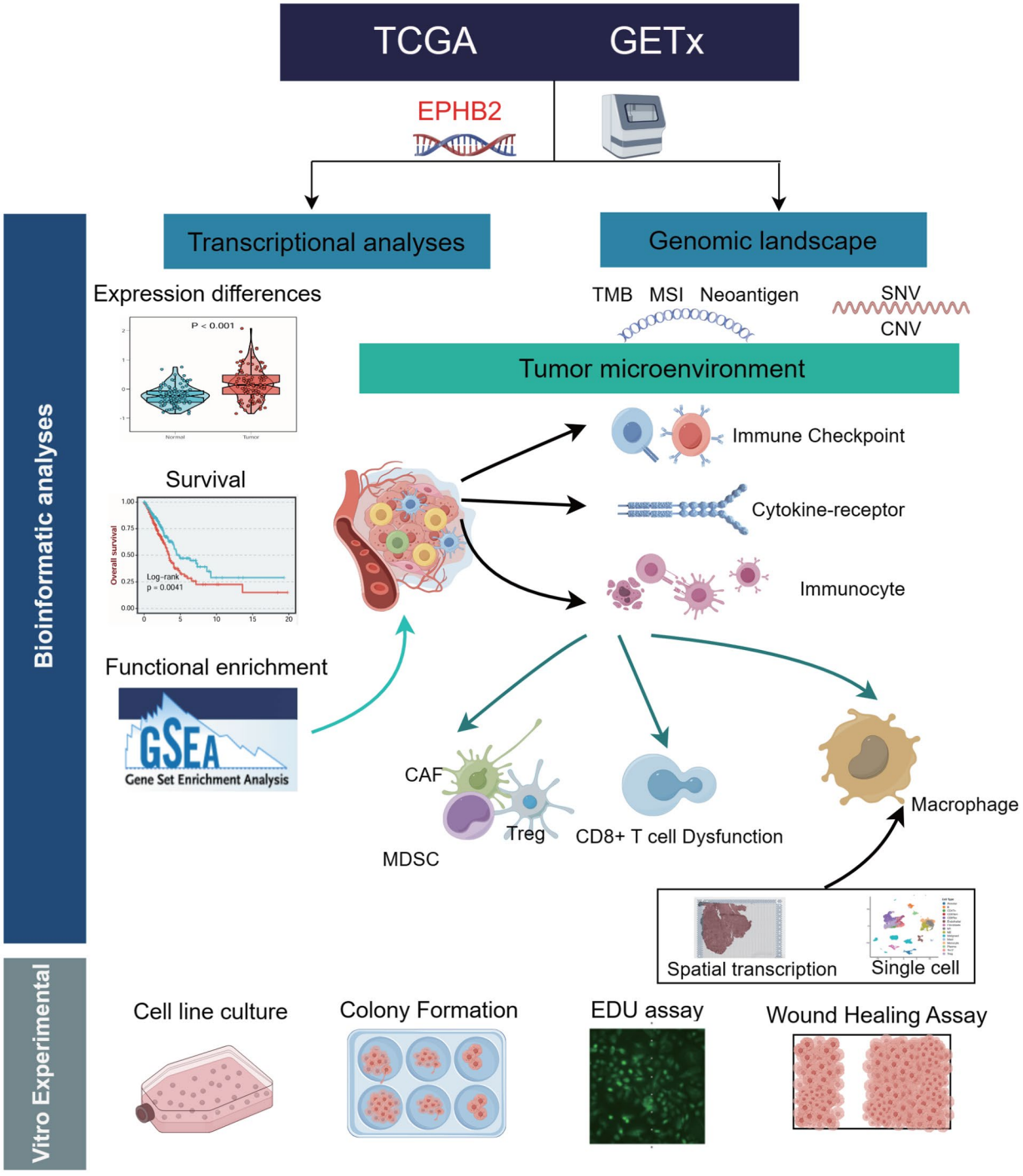

Fig. 1 Flowchart depicting the study's methodology

expression and tumor mutational burden (TMB) [23], microsatellite instability (MSI), and SNV.neoantigens.

Assessment of DNA mismatch repair, stemness, and epigenetic alterations

Relationships between EPHB2 expression, mismatch repair (MMR) genes [24], and DNA methyltransferases (DNMTs) [25] were visually analyzed. A previous study [26] was referenced to collect data on 15 homologous recombination repair (HRR) genes to examine their correlation with EPHB2 expression via the GEPIA2 tool [27].

DNA methylation-based stem score (DNAss) and RNA methylation-based stem score (RNAss) were calculated from methylation characteristics of each tumor

[28], and their correlations with EPHB2 mRNA expression were analyzed through heatmaps, focusing on genes modifying N1-methyladenosine (m1A), 5-methylcytosine (m5C), and N6-methyladenosine (m6A) [29].

Functional enrichment and interaction analyses

Protein-protein interaction data for EPHB2 were retrieved from ComPPI (https://comppi.linkgroup.hu/) and annotated through the "ID mapping" function of the UniProt database [30]. The "cor.test" function identified the top 200 genes co-expressed with EPHB2 for further analysis. Gene Ontology (GO) enrichment analyses for these genes were performed using the "clusterProfiler" package in R, with a significance threshold set at a false discovery rate-corrected P-value of below 0.05 [31, 32]. Additionally, Gene Set Enrichment Analysis (GSEA) was applied to quantitatively evaluate the functional enrichment of EPHB2 [33, 34].

Role of EPHB2 in immune function across cancers

We utilized the ESTIMATE algorithm to calculate the Immune, Stromal, and ESTIMATE scores across pan-cancer [35, 36]. EPHB2 expression was also assessed in tumors across six immunological subtypes using the TISIDB subtype module [37]. Samples were grouped based on high and low EPHB2 expression using median values. The distribution of the six immunological subtypes in these groups was examined using the chi-square test [38]. The influence of cytokine treatment on EPHB2 levels was evaluated using the Tumor Immune Syngeneic Mouse (TISMO) online tool [39]. The TIDE algorithm (http://tide.dfci.harvard.edu/) evaluated tumor immune evasion by examining cytotoxic T lymphocyte (CTL) dysfunction and exclusion [40]. Moreover, an independent immunotherapy cohort (PRJEB23709) was used to study the relationship between EPHB2 and the efficacy of immunotherapy in metastatic melanoma [41]. Various algorithms including CIBERSORT [42], quanTIseq [43], CIBERSORT-ABS [44], EPIC [45], xCell [46], TIMER [47], TIDE [48], and MCP-counter [49] quantified the proportions of immune cells infiltrating tumors, correlating these with EPHB2 expression through Spearman's correlation coefficients. We also explored the spatial correlations between EPHB2, the general macrophage marker CD68, and the M2 macrophage marker CD163 in lung adenocarcinoma (LUAD) using deconvolution analysis techniques. Initially, we gathered single-cell RNA sequencing data from samples of tumors diagnosed with LUAD (GSM5420754) sourced from the Gene Expression Omnibus (GEO, http://www.ncbi.nlm.nih.gov/geo), and then constructed a comprehensive scRNA reference library. To ensure the reliability of our analysis, we implemented stringent quality control measures on the single-cell transcriptome data, which included assessing the number of expressed genes, counting unique molecular identifiers (UMIs), and evaluating the percentage of mitochondrial RNA in each cell. Following this, we calculated the average expression of the top 25 specific genes for various cell types within the scRNA-seq reference data to create a signature score matrix. Finally, using the get_enrichment_matrix and enrichment_analysis functions from the "Cottrazm" R package, we successfully generated an enrichment score matrix, providing robust support for subsequent cell composition analysis. The expression landscape of genes in each micro-region was visualized using the SpatialFeaturePlot function from the "Seurat" R package. Expression of EPHB2 across multiple cancer types were conducted at the single-cell level using data from the Tumor Immune Single-cell Hub (TISCH) database [50]. EPHB2 mRNA expression data were sourced from multiple cell types across various datasets and were visualized using the "pHeatmap" R package. Additionally, Umap plots depicted EPHB2 expression across various cell types. The association between EPHB2 and 14 functional states in cancer was explored using the CancerSEA "correlation plot" module [51].

Connectivity map (cmap) analysis

Differential expression analysis between high and low EPHB2 expression identified the top 150 regulated genes in each cancer type. These genes formed an EPHB2-related signature used in Connectivity Map analyses to match with compound-related signatures from the CMAP_gene_signatures. RData file (https://www.pmgenomics.ca/bhklab/sites/default/files/downloads) [28, 52].

Molecular docking and molecular dynamics simulation

Molecular docking began with the preparation of the EPHB2 protein using AutoDock Tools, focusing on residue repair, hydrogen bond optimization, and energy minimization [53]. The ligand library was ionized and underwent energy minimization with Chem 3D 22.00. Virtual screening was conducted using AutoDock Vina 1.05.36, and the resultant figures were visualized using Pymol (Educational open source) [54].

Molecular dynamics simulations to examine the interactions between EPHB2 and small molecules were performed using Gromacs 2022.3 [55, 56]. Small molecules were prepared using AmberTools22 to apply the general amber force field (GAFF) force field, and Gaussian 16 W was used to add hydrogens and calculate restrained electrostatic potential (RESP) potentials. Simulations were conducted at a constant temperature of 300 K and pressure of 1 Bar using the Amber99sb-ildn force field in a Tip3p water solvent, with system charge neutralized by adding Na+ions. Energy minimization was followed by 100,000 steps each of isothermal isovolumic ensemble (NVT) and isothermal isobaric ensemble (NPT)

equilibration, with a coupling constant of 0.1 ps and duration of 100ps. A free molecular dynamics simulation ran for 5,000,000 steps with a step length of 2 fs, totaling 100ns. Post-simulation trajectory analysis was conducted to assess metrics such as root-mean-square variance (RMSD), protein rotation radius of each amino acid trajectory, solvent-accessible surface area (SASA), and root-mean-square fluctuation (RMSF).

Multiple fluorescence staining of LUAD paraffin sections

Multiple fluorescence staining was performed on LUAD paraffin sections to assess EPHB2 as a potential biomarker for M2 macrophages. The sections underwent deparaffinization, blocking with 5% bovine serum albumin. Samples were first incubated with primary antibodies: one group with EPHB2 (1:500, ImmunoWay) and CD163 (1:1000, ImmunoWay), and another group with EPHB2 (1:500, ImmunoWay) and CD68 (1:500, ImmunoWay). After treatment with appropriate secondary antibodies, nuclei were counterstained with DAPI, and slides were mounted using an antifade medium. Imaging was carried out with a confocal microscope (Pannoramic MIDI, 3DHistech), and the multispectral images were analyzed for cell-specific fluorescence using Caseviewer software (C.V 2.4).

Cell line culture and siRNA delivery

The PC9 lung adenocarcinoma cell line was cultured in 1640 medium with 10% fetal bovine serum (FBS, Servicebio) and 1% penicillin-streptomycin (Meilunbio) at 37°C in a 5% CO2 incubator (Heal Force). EPHB2 knockdown was executed using siRNA from GenePharma and Lipofectamine™ 2000 for transfection. The cells were seeded in 6-well plates, and siRNA was combined with Lipofectamine™ 2000 following manufacturer's protocol before being introduced to the cells. The cells were harvested 48 hours post-transfection for analysis of EPHB2 knockdown efficiency and to conduct proliferation and migration assays. The specific siRNA sequences used were: siEPHB2#1, sense 5'- ACCCGACTACACCAGCT TTAA-3'sense; siEPHB2#2, sense 5'- CTGGGTGGCCG CGTCATGAAA-3'.

RNA isolation and quantitative Real-time PCR (RT-PCR)

Total RNA was isolated using RNA fast200 (Fijie Reagent) following the manufacturer's guidelines. cDNA synthesis and qPCR were performed using Vazyme reagent. GAPDH served as the internal reference during experiments. The primer sequences for RT-PCR were: for GAPDH, forward 5'-GTCAGCCGCATCTTC TTT−3', reverse 5'-CGCCCAATACGACCAAAT −3'; and for EPHB2, forward 5'-CAACTGGCTACGGACCA AAT-3', reverse 5'- TCTCCATCCAGTTGGGAAAG-3'. Quantification of gene expression was carried out using the $2^{-\Delta\Delta Ct}$ method.

Colony Formation Assay

After transfection for 24 h, PC9 cells were seeded in 6-well plates at a density of 1000 cells per well and cultured for 7–14 days until colony formation, which were then processed with PBS, fixed with 4% polyoxymethylene for 30 min, and stained with 1% crystal violet for 10 min.

Wound Healing Assay

PC9 cells were seeded in 6-well plates at a concentration of 2.5×10^5 cells per well. After transfection with siEPHB2#1, siEPHB2#2, or siNC using the previously described siRNA delivery method, cells were allowed to confluence. A scratch was made in the cell layer using a 200 μL pipette tip, after which the medium was replaced with serum-free medium, and images were captured at 0 and 24 h using an inverted microscope.

Statistical analysis

Data analysis was conducted using SPSS (v23.0) and GraphPad Prism (version 8.0.1). Continuous variables were compared using the Student's t-test for normally distributed data and the Mann-Whitney U test for non-normal data. Chi-square and Fisher's exact tests were applied to categorical data comparisons. The prognostic value of EPHB2 levels was evaluated using univariate Cox regression analysis and the Kaplan-Meier method, considering a P-value below 0.05 as statistically significant.

Results

Pan-cancer analyses of EPHB2 expression

A comprehensive analysis of EPHB2 mRNA levels was performed using information sourced from the TCGA and GTEx databases, showing variable expression across 27 cancer types ($P<0.05$, Fig. 2A, Figure S1A). The CCLE data provided insights into EPHB2 expression levels across various cell lines, illustrated in Figure S1B. Furthermore, protein-level data from the CPTAC database indicated an elevation of EPHB2 in LUAD, lung squamous cell carcinoma (LUSC), glioblastoma multiforme (GBM), and pancreatic adenocarcinoma (PAAD) ($P<0.05$, Fig. 2B). A detailed evaluation of EPHB2 across pan-cancer, considering various clinical stages, subtypes, and TNM stages, is depicted in Figure S2 ($P<0.05$). This comprehensive analysis highlights the variable expression of EPHB2 across different cancer types and cellular contexts, underscoring its potential relevance in diverse oncological pathways.

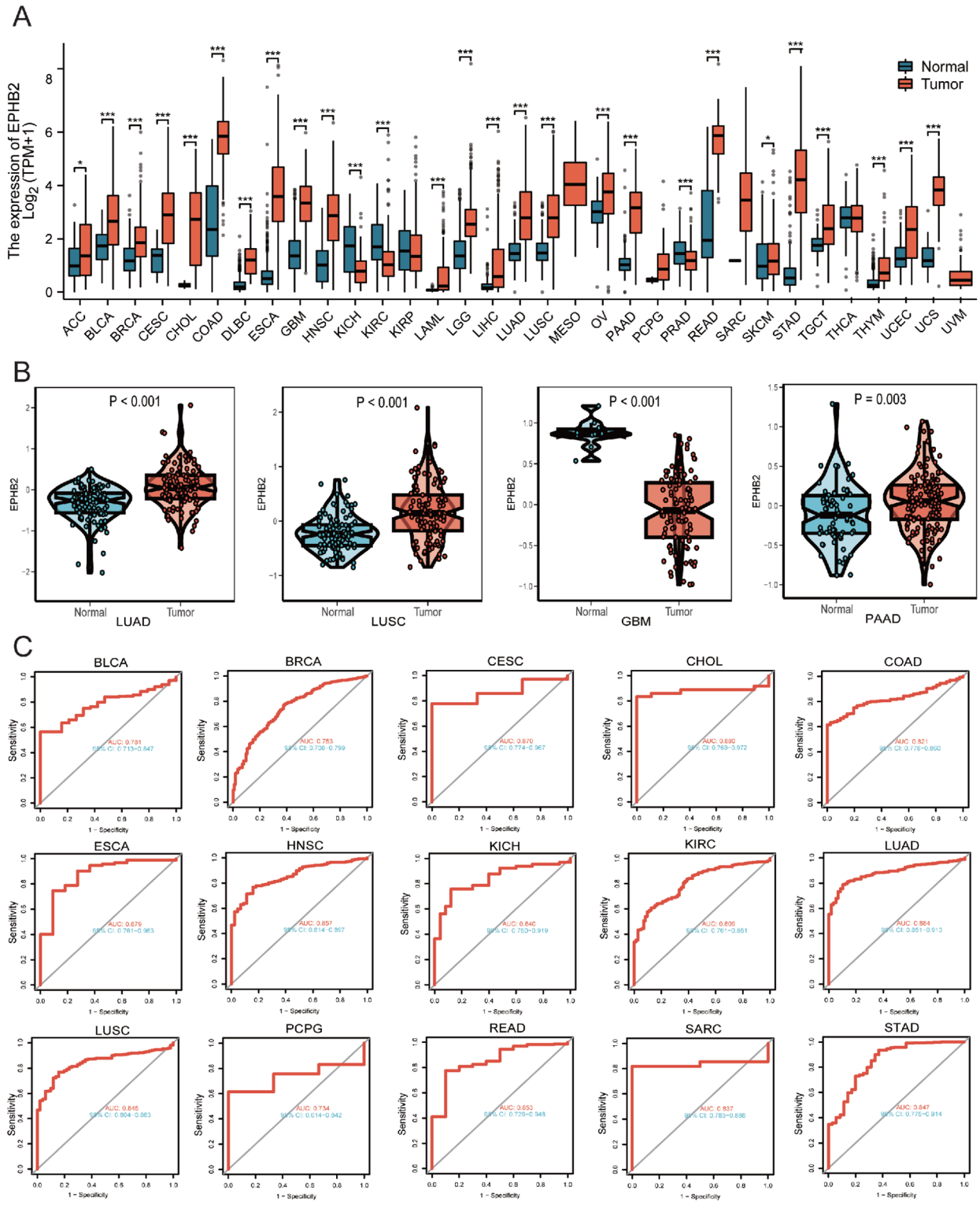

Fig. 2 Pan-cancer analysis of EPHB2 expression and its prognostic significance. **(A)** Comparison of EPHB2 levels in various cancer types versus normal tissues using data from TCGA and GTEx. **(B)** Comparative analysis of EPHB2 protein levels in lung adenocarcinoma (LUAD), lung squamous cell carcinoma (LUSC), glioblastoma (GBM), and pancreatic adenocarcinoma (PAAD) versus their normal counterparts, using data from CPTAC and HPA. **(C)** Diagnostic ROC curves across multiple cancers. Significance levels indicated as $*P < 0.05$, $**P < 0.01$, $***P < 0.001$; ns: not significant

The Diagnostic and Prognostic Value of EPHB2 across multiple Cancer types

ROC analysis highlighted the diagnostic potential of EPHB2 in multiple cancer types (Fig. 2C). The potential of EPHB2 as a prognostic marker was evaluated in 33 cancers from the TCGA database, examining its correlation with overall survival (OS), disease-specific survival (DSS), progression-free interval (PFI), and disease-free interval (DFI). Results from univariate Cox regression showed that high EPHB2 levels correlated with worse OS in uterine corpus endometrial carcinoma (UCEC), PAAD, kidney renal clear cell carcinoma (KIRC), ovarian serous cystadenocarcinoma (OV), GBM, brain lower grade glioma (LGG), LUAD, mesothelioma (MESO), uveal melanoma (UVM), and thymoma (THYM), but had a protective effect in skin cutaneous melanoma (SKCM), colon adenocarcinoma (COAD), rectum adenocarcinoma (READ) (Fig. 3A). In terms of DSS, EPHB2 emerged as a risk factor in various cancers including UCEC, kidney renal papillary cell carcinoma (KIRP), KIRC, OV, kidney chromophobe (KICH), LGG, MESO, pheochromocytoma and paraganglioma (PCPG), UVM, PAAD, and THYM, but was protective in SKCM and COAD (Fig. 3B). Regarding DFI, EPHB2 acted as a risk factor in PAAD but served a protective role in esophageal carcinoma (ESCA) (Fig. 3C). In terms of PFI, EPHB2 was identified as a risk factor in several cancers including UCEC, KIRC, OV, KICH, LGG, LUAD, PAAD, PCPG, UVM, and THYM, whereas it provided a protective effect in READ (Fig. 3D). Kaplan-Meier curves corroborated these findings (Fig. 3E and Figure S3-5). Collectively, these results suggest a general association between higher EPHB2 expression and poorer prognostic outcomes in patients with LUAD, UCEC, KIRC, PAAD, OV, MESO, LGG, UVM, and THYM.

Analysis of genomic changes and instability in EPHB2

We explored the genomic landscape of EPHB2, focusing on the prevalence of copy number variations (CNVs) and single nucleotide variations (SNVs). The COSMIC database was utilized to examine EPHB2 somatic mutations in 1591 cancer samples, identifying missense substitutions as the most prevalent mutation type at 32.62% (Fig. 4A). The cBioPortal tool revealed significant genetic alterations in EPHB2, especially in SKCM and UCEC cohorts (Fig. 4B). Notably, deep deletions of EPHB2 were predominantly observed in cholangiocarcinoma (CHOL), UVM, PCPG, THYM, KIRP and testicular germ cell tumors (TGCT). We also noted that the frameshift mutation starting at lysine (K) at 1020 positions of the EPHB2 protein had the most frequent mutation (Fig. 4C). An investigation into somatic copy number alteration (SCNA) frequencies indicated generally low frequency across most cancers (Fig. 4D). An analysis linking copy number alterations to EPHB2 expression demonstrated an increasing trend correlating with higher levels of genomic amplification ($P<0.001$, Fig. 4E). The relationships between EPHB2 and TMB, MSI, and SNV. neoantigens were also explored. A significant positive relationship was found between EPHB2 and TMB in UCEC, stomach adenocarcinoma (STAD), LUAD, liver hepatocellular carcinoma (LIHC), and head and neck squamous cell carcinoma (HNSC) (Fig. 4F), and between EPHB2 and MSI in sarcoma (SARC), bladder urothelial carcinoma (BLCA), and LUAD (Fig. 4G). Additionally, a notable positive relationship between EPHB2 and SNV. neoantigens was identified in cancers including THYM, PCPG, LUAD, LGG, and breast invasive carcinoma (BRCA) (Fig. 4H). Overall, these data underscored the significance of EPHB2 in the context of cancer genomic instability and immune response.

Correlation between EPHB2 expression, DNA repair, and stem-like properties in Cancer cells

The DNA damage response is critical for preserving genomic stability by repairing or removing faulty sequences and structures in chromosomes [57]. Cancer cells develop mechanisms such as MMR [58] and HRR [59] enhancing their abilities for self-renewal and stem-like characteristics [60]. We investigated how EPHB2 levels relate to the expression of MMR genes and HRR signatures, along with cancer stemness. Strong correlations were found between EPHB2 and multiple MMR genes across various cancers including TGCT, BLCA, LUAD, SARC, HNSC, UVM, cervical squamous cell carcinoma and endocervical adenocarcinoma (CESC), OV, PAAD, prostate adenocarcinoma (PRAD), SKCM, THYM, LIHC, PCPG, UCEC, uterine carcinosarcoma (UCS), and KIRP ($P<0.05$, Fig. 5A). Similarly, positive associations between EPHB2 expression and HRR signatures were observed in KIRP, UCEC, PCPG, BLCA, GBM, KIRC, LGG, adrenocortical carcinoma (ACC), LUAD, OV, MESO, UVM, PAAD, PRAD, lymphoid neoplasm diffuse large B-cell lymphoma (DLBC), STAD, thyroid carcinoma (THCA), READ, UCS, COAD, and KICH ($P<0.05$, Figure S6). Additionally, there was a positive association between EPHB2 and DNAss in THYM, and RNAss in READ ($P<0.05$, Fig. 5B, C). These results thus indicate EPHB2's involvement in DNA damage repair mechanisms.

Role of EPHB2 in epigenetic regulation

Epigenetic alterations play pivotal roles in cancer development and progression, and are significant targets for therapeutic intervention [61]. DNMTs, which catalyze DNA methylation, are involved in modulating tumor cell proliferation, differentiation, and survival [62]. EPHB2 expression demonstrated a significant negative

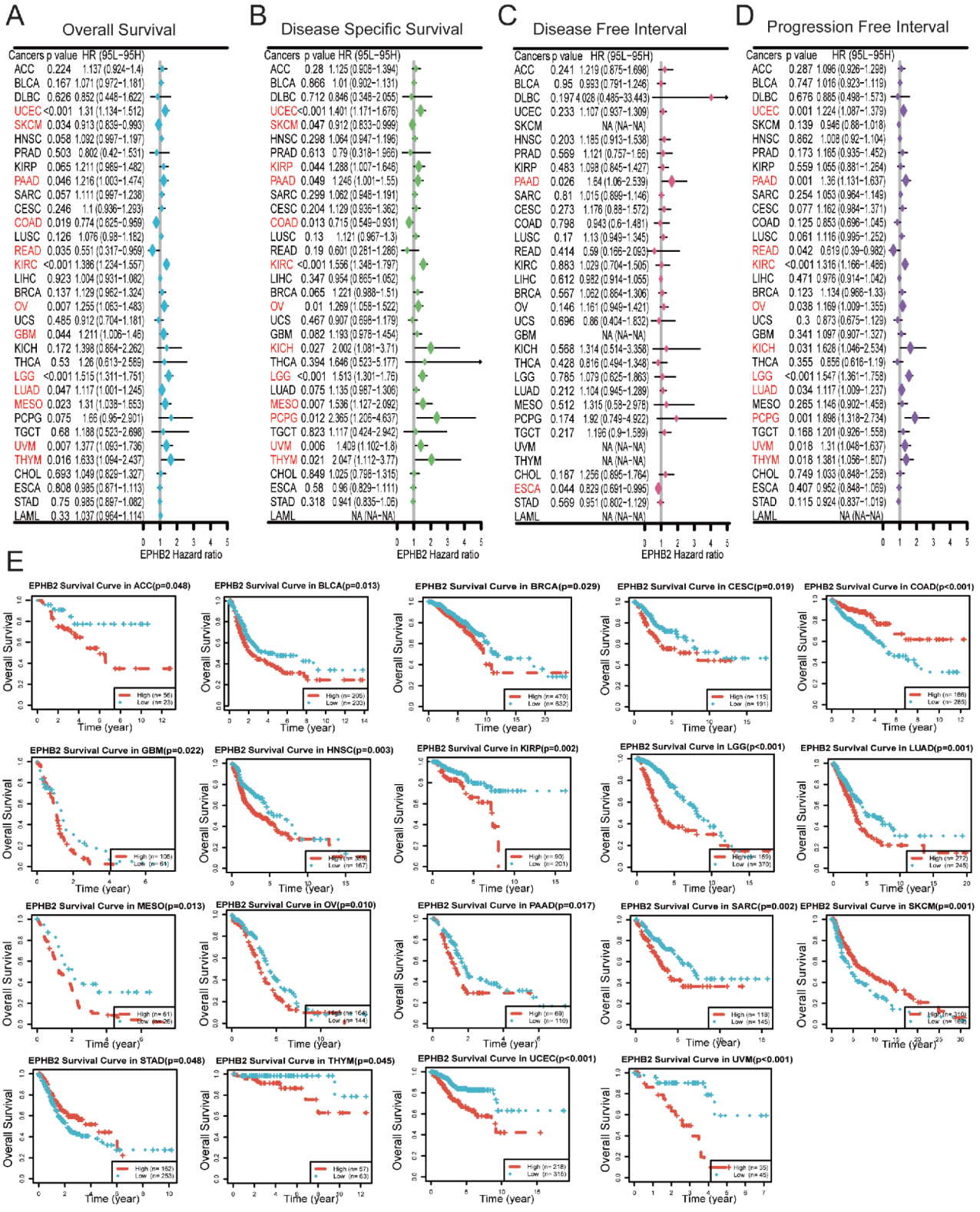

Fig. 3 Predictive significance of EPHB2 expression across cancers. **(A-D)** Forest plots showing the relationship of EPHB2 expression with overall survival (OS) **(A)**, disease-specific survival (DSS) **(B)**, disease-free interval (DFI) **(C)**, and progression-free interval (PFI) **(D)**. **(E)** Kaplan-Meier curves demonstrating the relationship between EPHB2 expression and OS for specified cancers

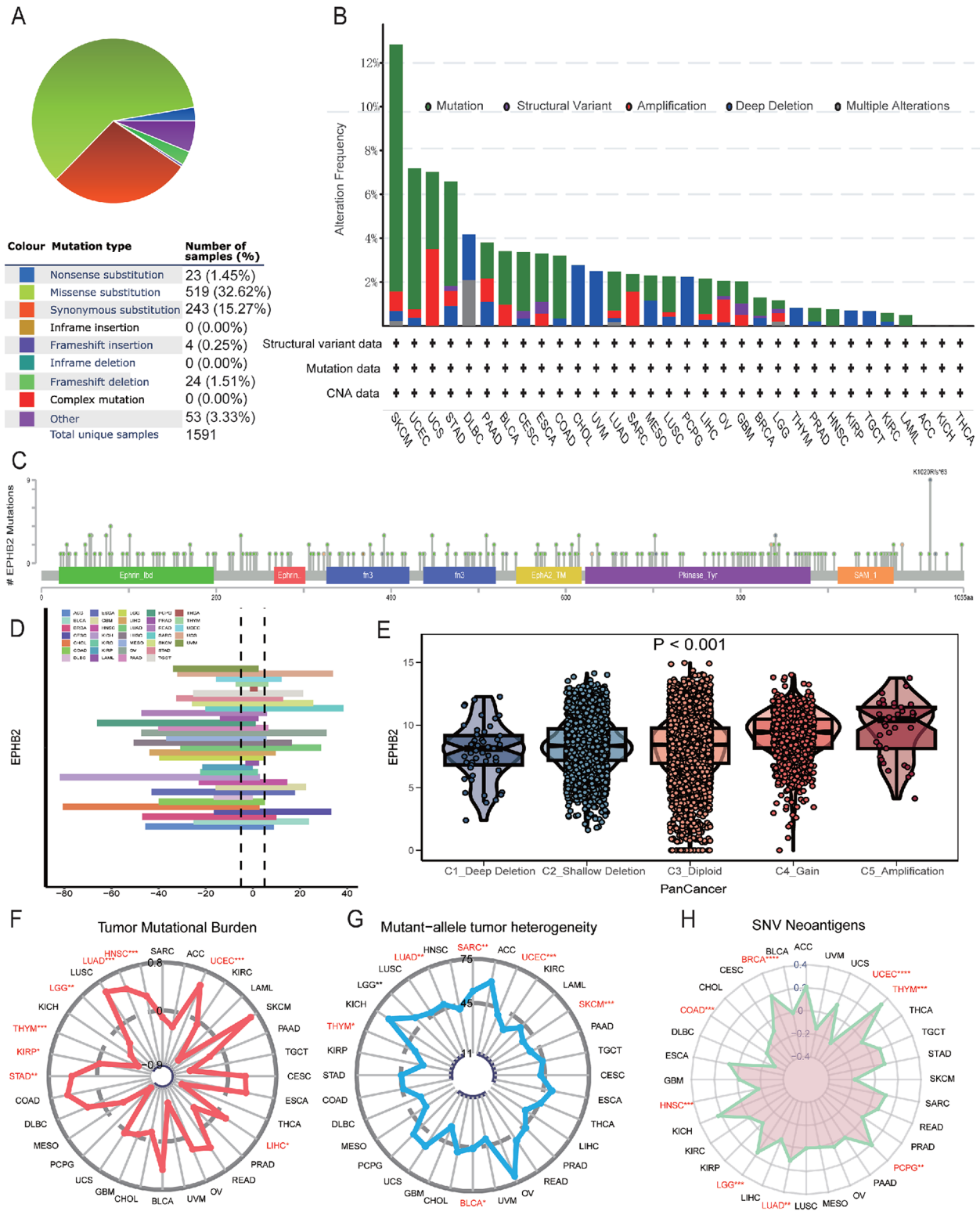

Fig. 4 EPHB2 mutational landscape in various cancers. **(A)** Types of EPHB2 mutations observed. **(B)** Prevalence of genetic alterations in EPHB2 across various cancers. **(C)** Mutation types and locations in EPHB2. **(D)** Distribution of EPHB2 somatic copy number alterations in each cancer type. **(E)** Analysis of EPHB2 expression differences across various copy number alteration types. Correlation studies between EPHB2 expression and tumor mutational burden (TMB) **(F)**, microsatellite instability (MSI) **(G)**, and SNV.neoantigens **(H)** using Spearman's correlation. Significance indicated as $^{*}P < 0.05$; $^{**}P < 0.01$; $^{***}P < 0.001$

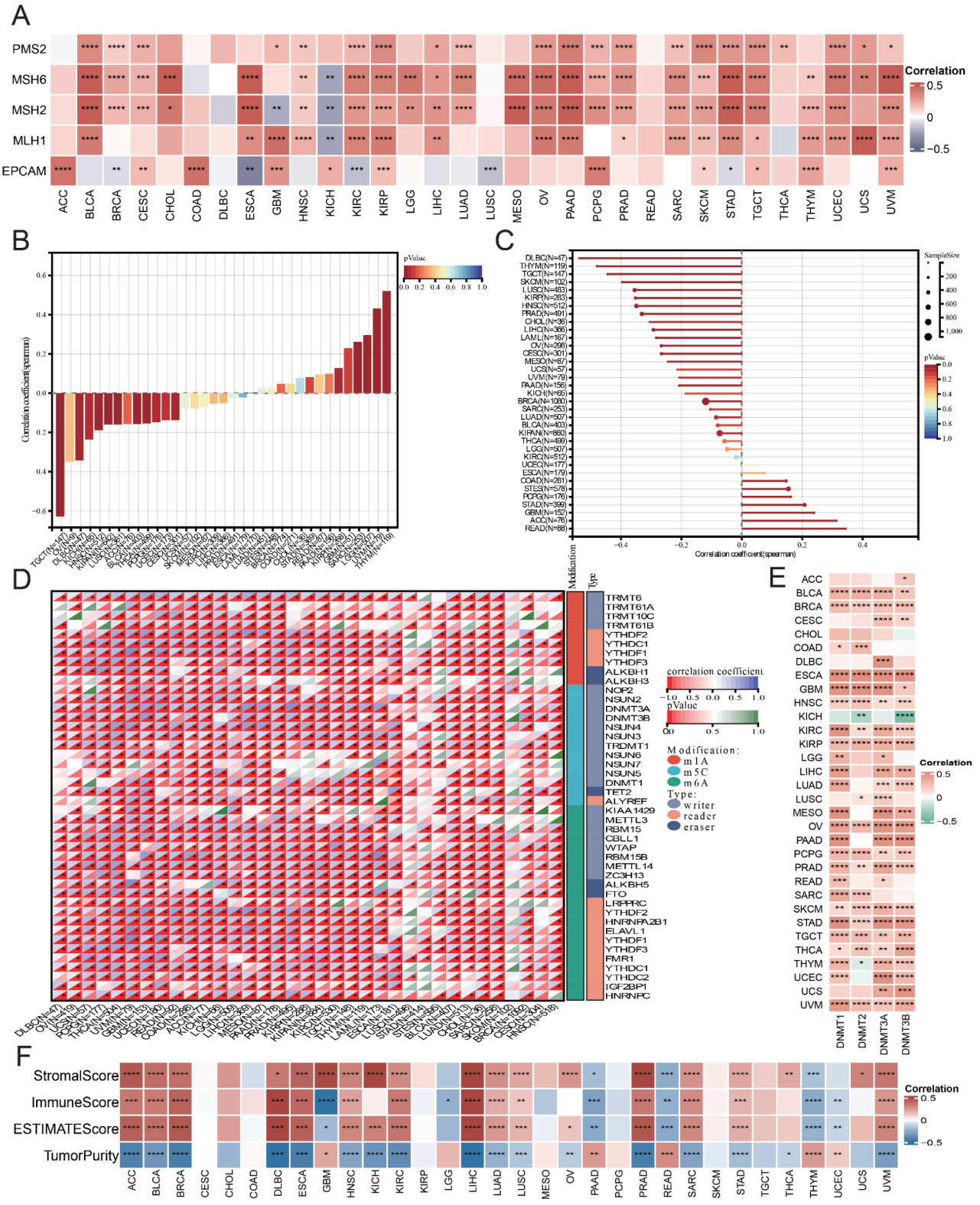

Fig. 5 Relationship between EPHB2 and mechanisms influencing cancer phenotype. **(A)** Heatmap showing associations of EPHB2 with five mismatch repair (MMR) genes across cancers. **(B)** Bar chart illustrating correlations between EPHB2 levels and DNA methylation-based stem score. **(C)** Lollipop chart depicting correlations between EPHB2 levels and RNA methylation-based stem score. **(D)** Heatmap presenting relationships between RNA modulations and EPHB2 expression in pan-cancer. **(E)** Heatmap of correlations between EPHB2 and four DNA methyltransferases (DNMTs). **(F)** Heatmap displaying relationships between EPHB2 expression and ESTIMATE, Immune, and Stromal scores. Significance levels indicated as $^{*}P < 0.05$, $^{**}P < 0.01$, $^{***}P < 0.001$, $^{****}P < 0.0001$

correlation with DNMT levels in KICH, while it was positively correlated in HNSC, BLCA, STAD, CESC, THCA, GBM, KIRC, LGG, LUSC, COAD, MESO, OV, LIHC, PCPG, LUAD, PRAD, KIRP, ESCA, READ, PAAD, SARC, SKCM, TGCT, UVM, BRCA, and UCS ($P<0.05$, Fig. 5E). Additionally, a negative relationship was observed between EPHB2 expression and methylation levels across multiple cancer types ($P<0.05$, Figure S7). The expression links between EPHB2 and various RNA modulating genes were also explored (Fig. 5D), highlighting EPHB2's extensive involvement in DNA methylation and RNA modification processes across diverse cancers.

EPHB2's connection to Immune responses and its role in Cancer pathways

Using data from the ComPPI website, the protein-protein interaction (PPI) network indicated that EPHB2's interactions occur in various cellular compartments including the cytosol and mitochondria (Fig. 6A). The "cor.test" function helped identify 200 genes that co-express with EPHB2, and GO enrichment analysis emphasized their significant roles in immune functions (Fig. 6B). Further, a comprehensive GSEA across multiple cancers provided deeper insights into the influence of EPHB2 on tumor prognosis by comparing gene expression profiles of patients with high versus low levels of EPHB2 (Fig. 6C). This analysis revealed that high expression of EPHB2 was strongly correlated with the activation of epithelial-mesenchymal transition (EMT) across several cancers. This relationship may account for the increased likelihood of lymph node, metastases, and recurrence in patients with elevated EPHB2 levels. The analysis also revealed differential enrichment in immune-related pathways in the heatmap clusters, including pathways for interferon-gamma (IFN-gamma), IFN-alpha, inflammatory responses, and cytokines like IL-6 and IL-12, as well as complement and allograft rejection pathways. Most notably, these pathways linked with high EPHB2 expression were observed to be less frequent in cancers such as COAD, READ, and STAD. Overall, these findings robustly demonstrate that EPHB2 expression is closely linked with enhanced proliferation, EMT, and immunosuppression in multiple cancer types.

EPHB2 and its Association with Immune Infiltration and Cytokine Dynamics in Cancer

Utilizing the ESTIMATE algorithm, we explored the relationship between EPHB2 expression and immune characteristics across 33 types of tumors. A significant positive association was found between ESTIMATE scores and immune scores in several cancers, notably in LUAD (Fig. 5F). Furthermore, immune subtypes C2 and C3 showed differential prevalence relative to EPHB2 expression levels, with C2 being dominant in the high EPHB2 group and C3 in the low EPHB2 group (Figure S8). Detailed correlations between EPHB2 and immune-related genes are illustrated in Figure S9. Using the TISMO tool, we analyzed the effects of cytokine treatments on EPHB2 expression in vitro, revealing elevated EPHB2 levels in the responder groups following cytokine treatment, particularly in lung cancer cell lines (Figure S10). Additionally, an independent immunotherapy cohort demonstrated that higher EPHB2 levels were associated with complete and partial responses to immune checkpoint blockade (ICB), contrasting with stable or progressive disease states ($P<0.01$, Fig. 7A). The TIDE score, a predictor of immunotherapy outcomes, was positively correlated with EPHB2 expression in 13 cancer types, including LUAD, indicating its potential as a marker for ICB treatment efficacy (Fig. 7B).

EPHB2 as an Indicator of M2 macrophage infiltration in Cancer

Further analysis aimed to clarify the link between EPHB2 expression and immune cell infiltration, revealing a positive correlation with M2 macrophage infiltration across various cancers (Figure S11 and Fig. 8E). Spatial transcriptomic analysis revealed a significant co-localization of EPHB2 expression with macrophage markers CD68 and CD163 in LUAD (Fig. 8F). Single-cell data from TISCH further confirmed EPHB2 presence in both macrophages and malignant cells across different cancers (Fig. 8A-D). These findings were supported by fluorescent staining, which clearly showed co-expression of EPHB2 with both CD68 and CD163 in LUAD tissue sections (Fig. 9A, B). Collectively, these data across bulk, spatial, single-cell transcriptional analyses, and fluorescence staining underscore a strong association between EPHB2 expression and M2 macrophage infiltration, proposing EPHB2 as a potential biomarker for M2 macrophage infiltration in pan-cancer.

Data from CancerSEA single-cell sequencing also explored correlations between EPHB2 expression and 14 functional states of cancer, revealing significant positive links with processes such as angiogenesis, EMT, inflammation, invasion, metastasis, quiescence, differentiation, apoptosis, and proliferation in LUAD (Figure S12). These findings highlight the multifaceted roles of EPHB2 in promoting oncogenic progression.

EPHB2's role in reducing LUAD Cell Proliferation and Migration

We investigated the impact of EPHB2 on malignant traits in LUAD using the PC9 cell lines. Knockdown of EPHB2 was verified via RT-PCR (Fig. 9C). Following EPHB2 silencing, notable reductions were observed in both cell proliferation and clone formation capabilities, as illustrated in Fig. 9D. Edu staining confirmed a substantial

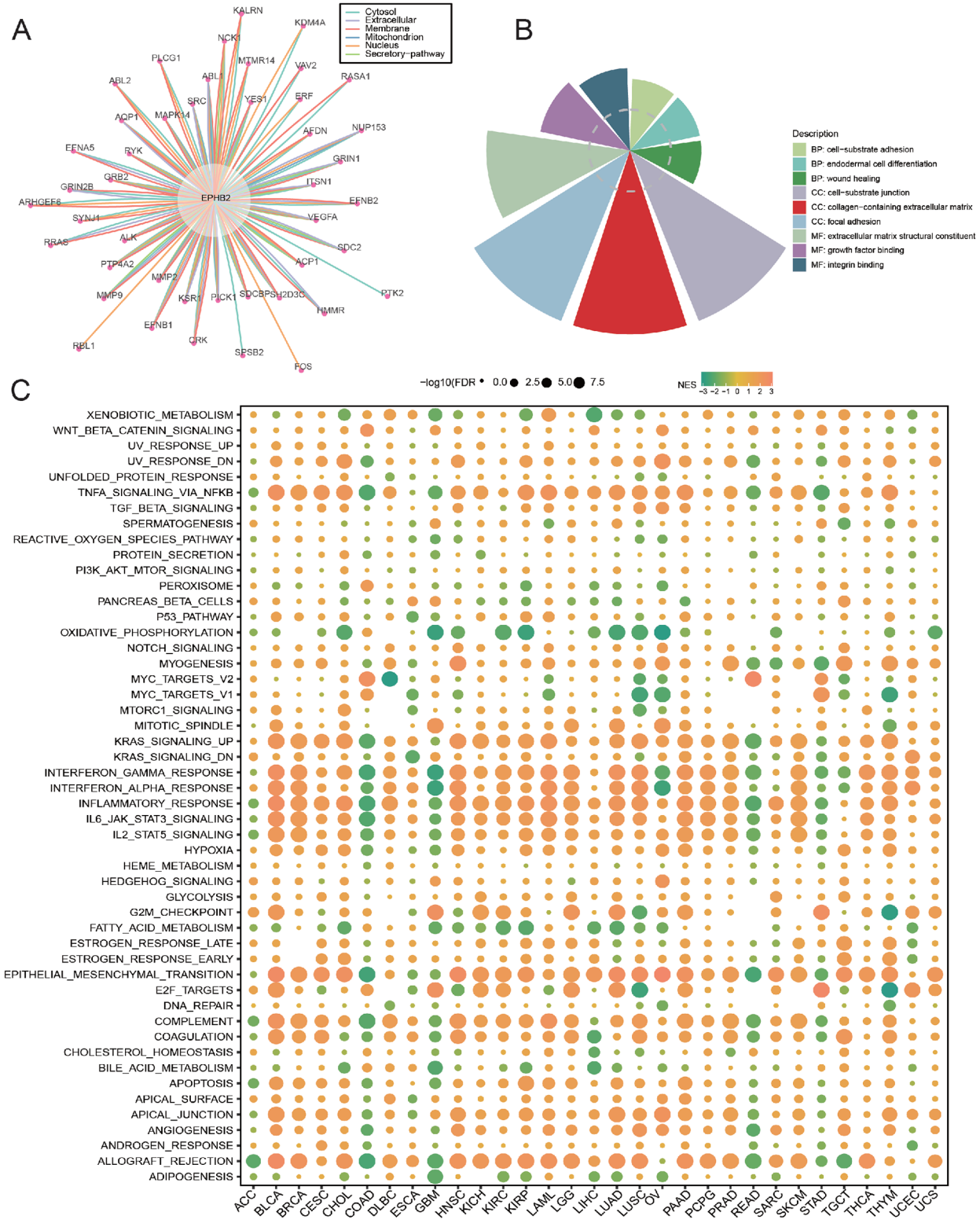

Fig. 6 Functional analysis of EPHB2 in oncology. **(A)** Displays the protein-protein interaction (PPI) network for proteins that interact with EPHB2. **(B)** GO pathway enrichment analysis for the top 200 genes co-expressed with EPHB2. **(C)** Bubble plot illustrating GSEA results comparing hallmark gene signatures between high and low EPHB2 expression groups across cancers

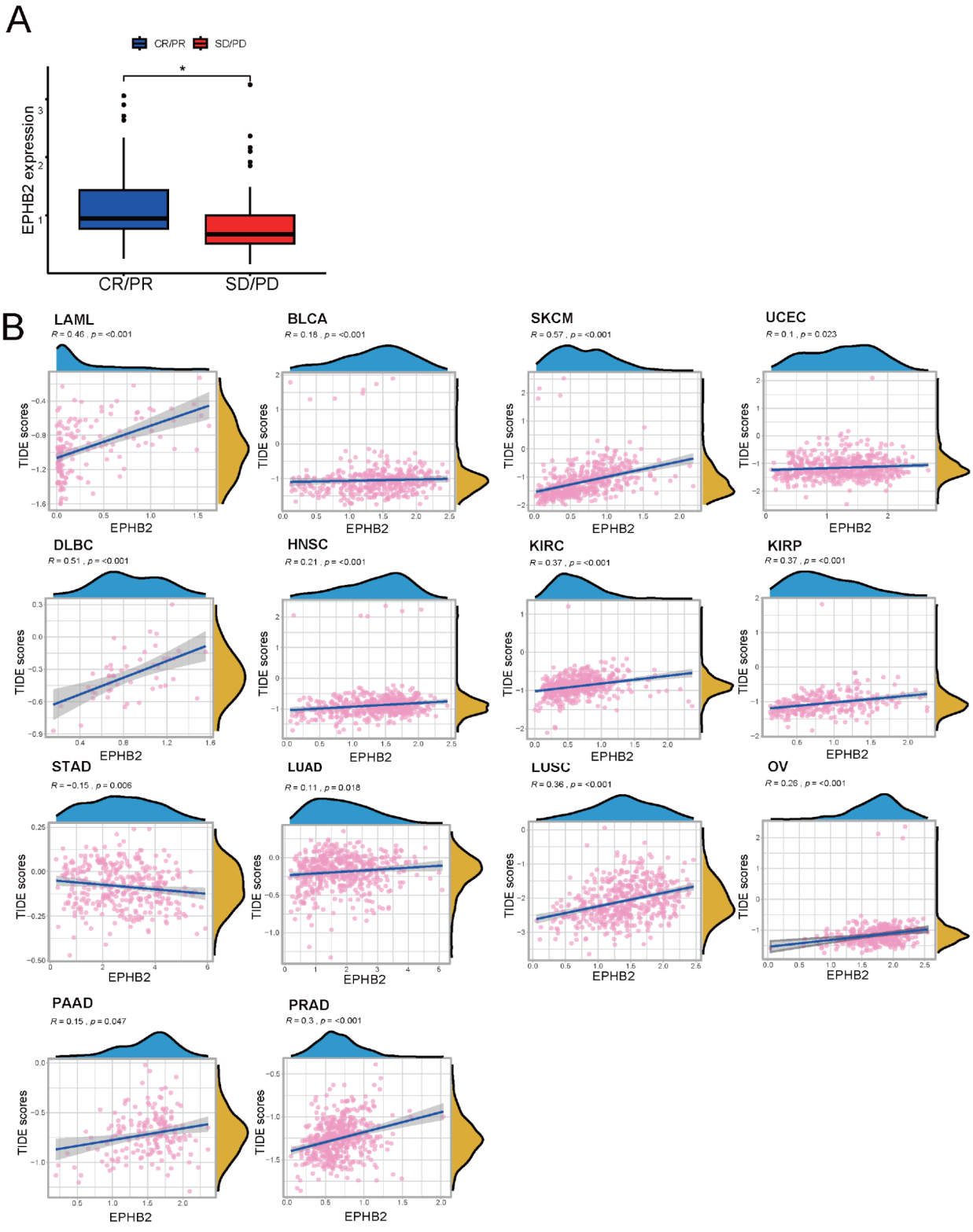

Fig. 7 Investigating EPHB2's impact on immunotherapy outcomes. **(A)** Box plots comparing EPHB2 expression with responses to immune checkpoint blockade in the PRJEB23709 cohort. **(B)** Spearman's correlation analysis depicting the association between EPHB2 levels and TIDE scores, validated by Student's t-test. Statistical significance indicated by $*P < 0.05$

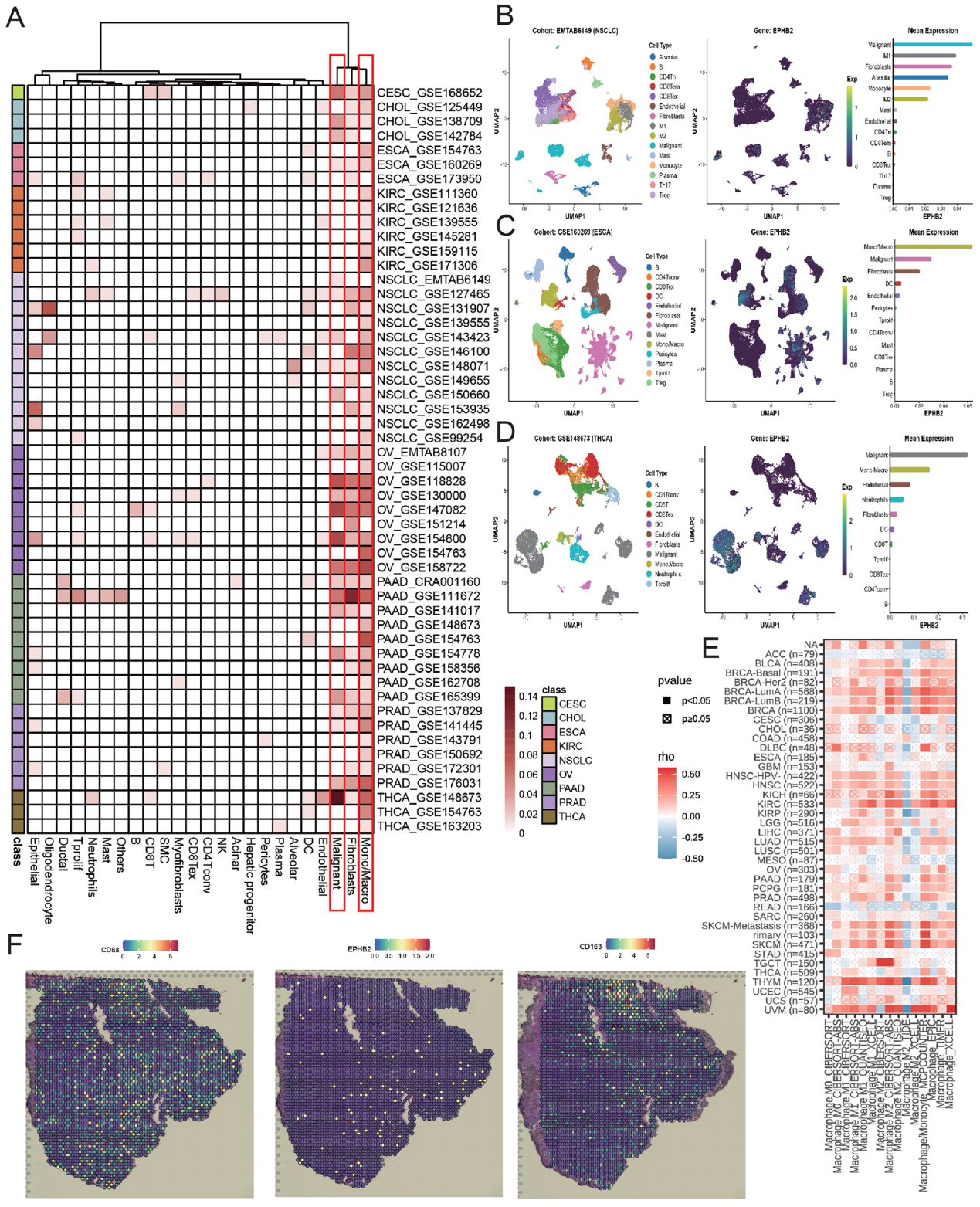

Fig. 8 EPHB2 as a marker for M2 macrophage infiltration across multiple cancers. **(A)** EPHB2 expression across cancer single-cell clusters from TISCH. Umap plots detail cell type distributions and EPHB2 intensity in non-small cell lung cancer (NSCLC) **(B)**, esophageal carcinoma (ESCA) **(C)**, and thyroid carcinoma (THCA) **(D)** tissues. **(E)** Analysis of the correlation between EPHB2 expression and macrophage infiltration in cancers using different algorithms. **(F)** Spatial transcriptomics to explore co-localization patterns of EPHB2, CD68, and CD163, with expression level-based color coding

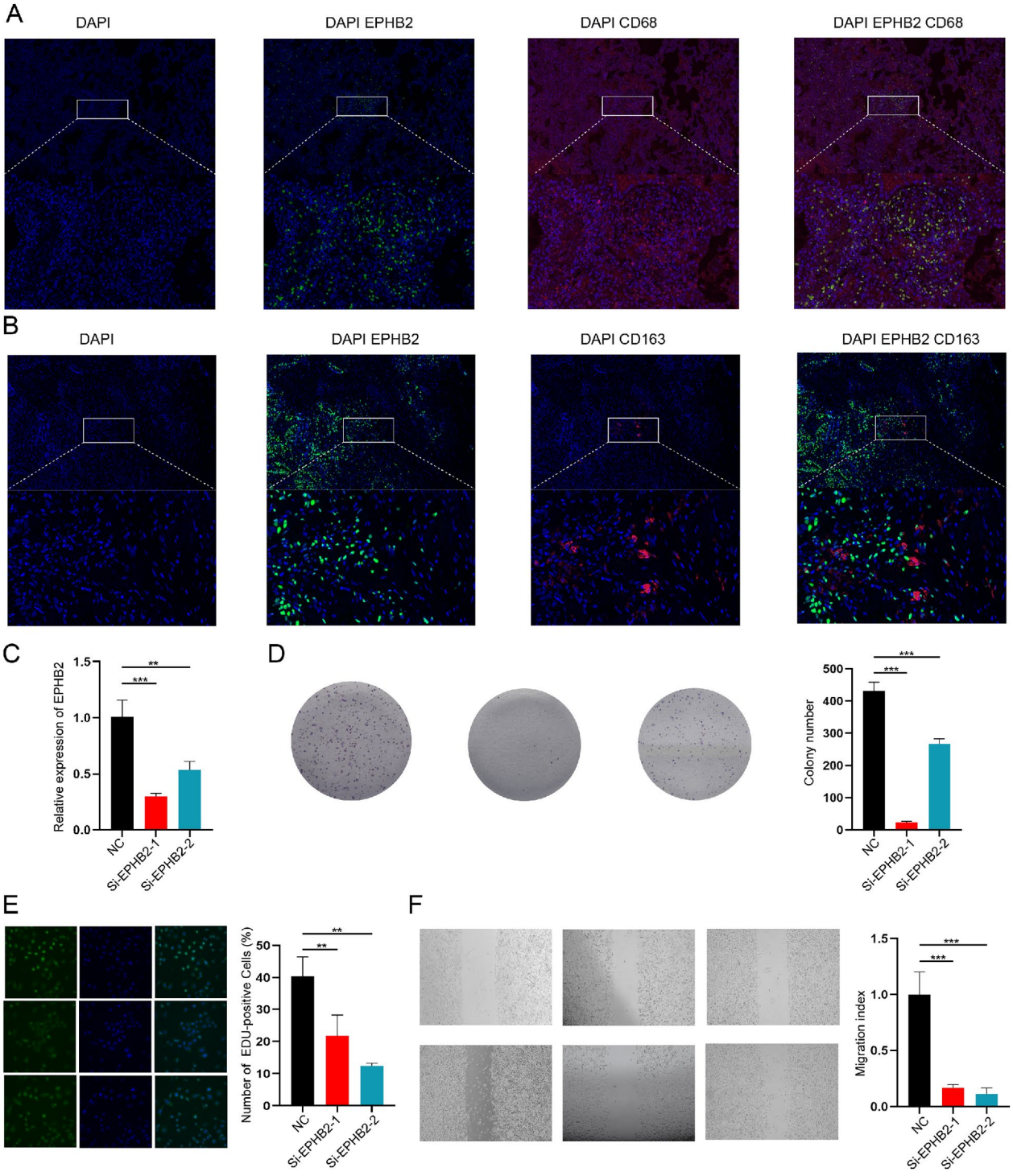

Fig. 9 Exploration of EPHB2's role in regulating malignancy in LUAD tumor cells. **(A)** Fluorescent images of tumor tissues stained for CD68 (red) and EPHB2 (green), with DAPI (blue) counterstaining. **(B)** Fluorescent images of tumor tissues stained for CD163 (red) or EPHB2 (green), with DAPI (blue) counterstaining. **(C)** EPHB2 mRNA levels in transfected cells. **(D, E)** Evaluation of EPHB2's effects on tumor cell proliferation using colony formation and EdU uptake assays. **(F)** Assessment of tumor cell migration post-EPHB2 knockdown via a wound healing assay. Significance denoted by $^{**}P < 0.01$, $^{***}P < 0.001$

decrease in LUAD cell proliferation following EPHB2 knockdown (Fig. 9E). Additionally, wound healing assays indicated that EPHB2 silencing compromised the migratory abilities of PC9 cells (Fig. 9F). Collectively, these findings confirm that knocking down EPHB2 significantly diminishes LUAD cell proliferation and migration, reinforcing the potential therapeutic relevance of targeting EPHB2 in cancer treatment strategies.

10 Molecular Docking and Dynamics of EPHB2-Targeting compounds

Identifying compounds that can effectively modulate EPHB2 activity is crucial for therapeutic development. Using the cMap tool, we identified W.13 as a compound that could potentially reverse EPHB2's dysregulated molecular traits and mitigate its oncogenic effects (Fig. 10A). To evaluate the potential interaction between the EPHB2 protein and W.13, a molecular docking analysis was performed. Ten EPHB2 models were developed using alphaFold2.0, based on the FASTA sequence provided (Supplementary Material 1). The model with the highest ranking demonstrated an overall quality factor of 82.69. AutoDock Vina 1.05.36 showed successful docking of W.13 to EPHB2 (DockScore: -6.148 kcal/mol) (Fig. 10B), indicating W.13's potential to activate EPHB2.

Subsequent molecular dynamics simulations were conducted to assess the stability of the W.13-EPHB2 complex. The root mean square deviation (RMSD) curve stabilized between 20 and 100 ns, indicating strong stability with minimal structural changes, as the RMSD plateaued around 1.8 nm (Fig. 10C). Analysis of root mean square fluctuation (RMSF) highlighted increased flexibility at certain EPHB2 residues when bound to W.13, specifically between residues SER A 102 to CYS A 107, LYS A 476 to TYR A 504, and SER A 898 to LEU A 905, as indicated by elevated RMSF values (Fig. 10D). The radius of gyration (Rg) remained consistent at about 5.1 nm during the simulation, suggesting that the complex maintained a stable conformation (Fig. 10E). Hydrogen bond dynamics within the W.13-EPHB2 complex were also monitored, maintaining between 2 and 3 bonds, with peaks of up to 5 at certain intervals (Fig. 10F). These insights suggest that the interaction between small molecules and protein receptors is not merely static but constitutes a dynamic and variable network of interactions where hydrogen bonds are continuously formed and broken, yet overall remain within a relatively stable range. This reflects the complexity and sophistication of biomolecular interactions. Additionally, solvent-accessible surface area (SASA) measurements stabilized around 575 square nanometers after initial fluctuations, indicating stable interactions of the complex (Fig. 10G). These insights underscore the dynamic interactions between the small molecule and protein receptor, providing valuable information for future therapeutic development.

Discussion

Recent studies have indicated that EPHB2 plays a role in the proliferation and migration of several cancer types, including GBM, CHOL, CESC, LUAD, and STAD, with its expression inversely related to prognosis [8, 10–13]. The use of bioinformatics and comprehensive cancer analyses using publicly available datasets provides insights into the role of molecular factors in tumorigenesis and progression. However, a comprehensive investigation specifically targeting EPHB2 across pan-cancer has not yet been conducted. Therefore, we examined EPHB2's gene expression, survival rates, methylation patterns, genetic variations, and immune infiltration across multiple cancers, complemented by in vitro cellular experiments to investigate its potential impact on cancer.

In several cancers, including LUAD, UCEC, KIRC, PAAD, OV, MESO, LGG, YVM, and THYM, EPHB2 acts as a prognostic risk factor, whereas in SKCM, COAD, and READ, it serves as a protective factor. This reflects the activation of distinct molecular pathways across various cancers, highlighting the complexity and diversity inherent in cancer biology [63]. Moreover, our findings indicate that higher EPHB2 expression levels are associated with advanced TNM stages in UCEC, KIRC, MESO, and THYM, corroborated by GESA results. These findings reinforce the utility of EPHB2 expression levels as a reliable biomarker for cancer prognosis.

In GO enrichment analyses, EPHB2 was associated with key immune functions, notably the regulation of the innate immune response and cytokine signaling pathways. Among six immunological subtypes analyzed, the C2 subtype, dominated by IFN-γ, was predominant in the high EPHB2 expression group. IFN-γ is crucial for initiating immune responses, tumor immunosurveillance, and maintaining normal tissue homeostasis [64]. The GSEA results also suggest that EPHB2 may affect tumor progression by modulating IFN-α and IFN-γ responses, revealing a previously unreported mechanism that could guide future research directions.

Immunotherapy in clinical settings frequently employs immune checkpoint inhibitor (ICI) drugs, such as antibodies targeting CTLA-4, PD-1, and PD-L1, which are highly effective. Tumor mutational burden (TMB) and microsatellite instability (MSI) are indicators that help predict the likelihood of tumor response to these therapies, with higher levels typically indicating better response to ICIs [65–67]. In this context, EPHB2 expression positively correlated with TMB, MSI, and immune checkpoint markers across several studied cancer types. Analysis of a cohort treated with anti-PD1 alone or in combination with anti-CTLA4 showed that individuals

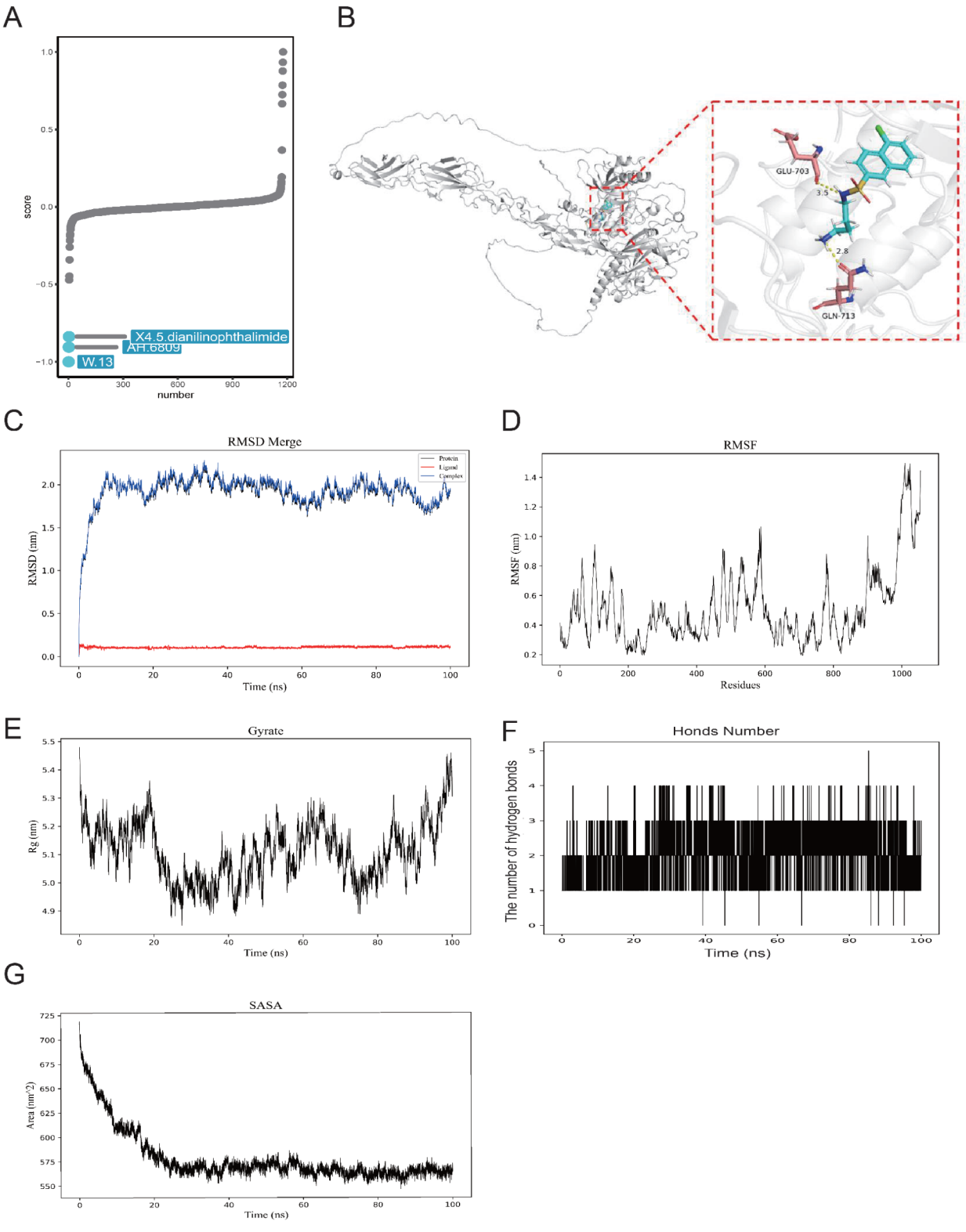

Fig. 10 Molecular interactions and dynamics of EPHB2. **(A)** Identification of EPHB2-targeting compounds through cMap analysis. **(B)** 3D molecular docking illustrations of EPHB2 with compound W.13. **(C-G)** Stability assessments of the W.13-EPHB2 complex using metrics such as root-mean-square deviation (RMSD), root-mean-square fluctuation (RMSF), radius of gyration (Rg), hydrogen bond dynamics, and solvent-accessible surface area (SASA)

with higher EPHB2 levels tended to have a better treatment response. Furthermore, existing research suggests that combining EPHB2 and PD-1 blockade might be an effective approach for treating metastatic urothelial carcinoma, indicating that EPHB2 could be a vital marker for assessing the immune status of tumors [68].

Analysis of immunomodulatory functions revealed a significant link between EPHB2 expression and the Immune scores, suggesting EPHB2's role in influencing the tumor microenvironment. Higher EPHB2 levels were also positively associated with M2 macrophage infiltration in bulk and single-cell transcriptomic, with immunofluorescence confirming this association. Moreover, we focused on the identification of potential EPHB2-activating drugs. This exploration is pivotal as it might lead to new therapeutic strategies that could improve current treatments. The potential clinical applications of EPHB2 as a biomarker are significant. By quantifying variations in EPHB2 expression, oncologists may be able to better stratify patients into more precise risk categories, thus refining treatment protocols. For instance, higher EPHB2 levels, associated with poor prognosis in several cancers, might advocate for the adoption of more aggressive treatment regimens. Conversely, in cancers such as colorectal adenocarcinoma (COAD) and rectal adenocarcinoma (READ), where EPHB2 plays a protective role, the prognosis might support less intensive treatment options. Furthermore, the functionality of EPHB2 as a biomarker could extend to improving the prediction of patient responses to immunotherapy, suggesting a pathway toward more personalized treatment approaches that could favorably impact patient outcomes. Despite the comprehensive nature of this study, it presents certain limitations that merit attention. The lack of a detailed pathway analysis constrains a deeper understanding of the specific mechanisms through which EPHB2 exerts its varied influences across different cancer contexts. Further, while the study effectively outlines EPHB2's roles within cancer pathology and its interaction with the tumor microenvironment and immune responses, it does not extensively delve into the direct mechanisms underlying these relationships. Future research should aim to elaborate on the mechanistic pathways involving EPHB2, potentially through longitudinal studies that could offer insights into the temporal dynamics of EPHB2 in cancer progression. Such studies would enhance the understanding of EPHB2's roles and facilitate the development of targeted therapies that leverage its biomarker potential.**5 Conclusion**.

This study represents the first comprehensive pan-cancer analysis of EPHB2, establishing its significant role as a predictive biomarker for both prognosis and immunotherapy efficacy. Our findings illuminate EPHB2's critical involvement in cancer immunity, particularly as a marker for M2 macrophage infiltration across a variety of cancer types. Furthermore, we identified a potential compound that could lead to new therapeutic strategies. These future research efforts are expected to broaden our comprehension of EPHB2's implications in oncology and underscore its value as a therapeutic target.

Supplementary Information

The online version contains supplementary material available at https://doi.org/10.1186/s12885-024-12843-0.

Supplementary Material 1
Supplementary Material 2
Supplementary Material 3
Supplementary Material 4
Supplementary Material 5
Supplementary Material 6
Supplementary Material 7
Supplementary Material 8
Supplementary Material 9
Supplementary Material 10
Supplementary Material 11
Supplementary Material 12
Supplementary Material 13
Supplementary Material 14

Acknowledgements
The schematic diagram of the graphical abstract was drawn by Figdraw.

Author contributions
Shengshan Xu and Zhuming Lu conceptualized and designed the study. Shengshan Xu, Youbin Zheng, Min Ye, Tao Shen, Dongxi Zhang, and Zumei Li performed the data analyses and prepared the figures and tables. Shengshan Xu, Youbin Zheng, Min Ye, and Zhuming Lu wrote and revised the manuscript. All authors contributed to the article and approved the submitted version.

Funding
This work was supported by the Technology Project of Jiangmen (Nos. 2220002000183, 2320002000933) and the Medical Science Foundation of Jiangmen Central Hospital (J202401).

Data availability
The original contributions presented in the study are included in the article/Supplementary Material. Further inquiries can be directed to the corresponding authors.

Declarations

Ethics approval and consent to participate
This study was performed in line with the principles of the Declaration of Helsinki. The studies involving human participants were reviewed and approved by The Clinical Research Ethics Committee of Jiangmen Central Hospital (Approval number: 2022-98). The patients/participants provided their written informed consent to participate in this study.

Consent for publication
Not applicable.

Competing interests
The authors declare no competing interests.

Received: 10 July 2024 / Accepted: 22 August 2024
Published online: 28 August 2024

References

1. Sung H, Ferlay J, Siegel RL, Laversanne M, Soerjomataram I, Jemal A, Bray F. Global Cancer statistics 2020: GLOBOCAN estimates of incidence and Mortality Worldwide for 36 cancers in 185 countries. CA Cancer J Clin. 2021;71(3):209–49.
2. Srivastava S, Koay EJ, Borowsky AD, De Marzo AM, Ghosh S, Wagner PD, Kramer BS. Cancer overdiagnosis: a biological challenge and clinical dilemma. Nat Rev Cancer. 2019;19(6):349–58.
3. Xu S, Chen X, Fang J, Chu H, Fang S, Zeng L, Ma H, Zhang T, Chen Y, Wang T, et al. Comprehensive analysis of 33 human cancers reveals clinical implications and immunotherapeutic value of the solute carrier family 35 member A2. Front Immunol. 2023;14:1155182.
4. Birnboim-Perach R, Benhar I. Using combination therapy to overcome diverse challenges of Immune checkpoint inhibitors treatment. Int J Biol Sci. 2024;20(10):3911–22.
5. Holder N, Klein R. Eph receptors and ephrins: effectors of morphogenesis. Development. 1999;126(10):2033–44.
6. Mann F, Peuckert C, Dehner F, Zhou R, Bolz J. Ephrins regulate the formation of terminal axonal arbors during the development of thalamocortical projections. Development. 2002;129(16):3945–55.
7. Wilkinson DG. Eph receptors and ephrins: regulators of guidance and assembly. Int Rev Cytol. 2000;196:177–244.
8. Qiu W, Song S, Chen W, Zhang J, Yang H, Chen Y. Hypoxia-induced EPHB2 promotes invasive potential of glioblastoma. Int J Clin Exp Pathol. 2019;12(2):539–48.
9. Farshchian M, Nissinen L, Siljamäki E, Riihilä P, Toriseva M, Kivisaari A, Ala-Aho R, Kallajoki M, Veräjänkorva E, Honkanen HK, et al. EphB2 promotes progression of cutaneous squamous cell carcinoma. J Invest Dermatol. 2015;135(7):1882–92.
10. Khansaard W, Techasen A, Namwat N, Yongvanit P, Khuntikeo N, Puapairoj A, Loilome W. Increased EphB2 expression predicts cholangiocarcinoma metastasis. Tumour Biology: J Int Soc Oncodevelopmental Biology Med. 2014;35(10):10031–41.
11. Gao Q, Liu W, Cai J, Li M, Gao Y, Lin W, Li Z. EphB2 promotes cervical cancer progression by inducing epithelial-mesenchymal transition. Hum Pathol. 2014;45(2):372–81.
12. Zhao C, Wang A, Lu F, Chen H, Fu P, Zhao X, Chen H. Overexpression of junctional adhesion molecule-A and EphB2 predicts poor survival in lung adenocarcinoma patients. Tumour Biology: J Int Soc Oncodevelopmental Biology Med. 2017;39(2):1010428317691000.
13. Yin J, Li Z, Ye L, Birkin E, Li L, Xu R, Chen G, Ji J, Zhang Z, Jiang WG, et al. EphB2 represents an independent prognostic marker in patients with gastric cancer and promotes tumour cell aggressiveness. J Cancer. 2020;11(10):2778–87.
14. Sikkema AH, den Dunnen WF, Hulleman E, van Vuurden DG, Garcia-Manero G, Yang H, Scherpen FJ, Kampen KR, Hoving EW, Kamps WA, et al. EphB2 activity plays a pivotal role in pediatric medulloblastoma cell adhesion and invasion. Neurooncology. 2012;14(9):1125–35.
15. Jang BG, Kim HS, Chang WY, Bae JM, Kang GH. Prognostic significance of EPHB2 expression in Colorectal Cancer Progression. J Pathol Translational Med. 2018;52(5):298–306.
16. Goldman MJ, Craft B, Hastie M, Repečka K, McDade F, Kamath A, Banerjee A, Luo Y, Rogers D, Brooks AN, et al. Visualizing and interpreting cancer genomics data via the Xena platform. Nat Biotechnol. 2020;38(6):675–8.
17. Barretina J, Caponigro G, Stransky N, Venkatesan K, Margolin AA, Kim S, Wilson CJ, Lehár J, Kryukov GV, Sonkin D, et al. The Cancer Cell Line Encyclopedia enables predictive modelling of anticancer drug sensitivity. Nature. 2012;483(7391):603–7.
18. Cerami E, Gao J, Dogrusoz U, Gross BE, Sumer SO, Aksoy BA, Jacobsen A, Byrne CJ, Heuer ML, Larsson E, et al. The cBio cancer genomics portal: an open platform for exploring multidimensional cancer genomics data. Cancer Discov. 2012;2(5):401–4.
19. Yuan Q, Lu X, Guo H, Sun J, Yang M, Liu Q, Tong M. Low-density lipoprotein receptor promotes crosstalk between cell stemness and tumor immune microenvironment in breast cancer: a large data-based multi-omics study. J Transl Med. 2023;21(1):871.
20. Chandrashekar DS, Karthikeyan SK, Korla PK, Patel H, Shovon AR, Athar M, Netto GJ, Qin ZS, Kumar S, Manne U, et al. UALCAN: an update to the integrated cancer data analysis platform. Neoplasia (New York NY). 2022;25:18–27.
21. Wei T, Liu J, Ma S, Wang M, Yuan Q, Huang A, Wu Z, Shang D, Yin P. A nucleotide metabolism-related gene signature for risk stratification and prognosis prediction in Hepatocellular Carcinoma based on an Integrated Transcriptomics and Metabolomics Approach. Metabolites 2023, 13(11).
22. Tate JG, Bamford S, Jubb HC, Sondka Z, Beare DM, Bindal N, Boutselakis H, Cole CG, Creatore C, Dawson E, et al. COSMIC: the catalogue of somatic mutations in Cancer. Nucleic Acids Res. 2019;47(D1):D941–7.
23. Wang Z, Yuan Q, Chen X, Luo F, Shi X, Guo F, Ren J, Li S, Shang D. A prospective prognostic signature for pancreatic adenocarcinoma based on ubiquitination-related mRNA-lncRNA with experimental validation in vitro and vivo. Funct Integr Genomics. 2023;23(3):263.
24. Latham A, Srinivasan P, Kemel Y, Shia J, Bandlamudi C, Mandelker D, Middha S, Hechtman J, Zehir A, Dubard-Gault M, et al. Microsatellite instability is Associated with the Presence of Lynch Syndrome Pan-cancer. J Clin Oncology: Official J Am Soc Clin Oncol. 2019;37(4):286–95.
25. Lyko F. The DNA methyltransferase family: a versatile toolkit for epigenetic regulation. Nat Rev Genet. 2018;19(2):81–92.
26. Wu S, Zhang Y, Zhang Y, Chen LH, Ouyang HF, Xu X, Du Y, Ti XY. Mutational landscape of homologous recombination-related genes in small-cell lung cancer. Cancer Med. 2023;12(4):4486–95.
27. Tang Z, Kang B, Li C, Chen T, Zhang Z. GEPIA2: an enhanced web server for large-scale expression profiling and interactive analysis. Nucleic Acids Res. 2019;47(W1):W556–60.
28. Malta TM, Sokolov A, Gentles AJ, Burzykowski T, Poisson L, Weinstein JN, Kamińska B, Huelsken J, Omberg L, Gevaert O, et al. Machine learning identifies stemness features Associated with Oncogenic Dedifferentiation. Cell. 2018;173(2):338–e354315.
29. Shi H, Chai P, Jia R, Fan X. Novel insight into the regulatory roles of diverse RNA modifications: re-defining the bridge between transcription and translation. Mol Cancer. 2020;19(1):78.
30. Veres DV, Gyurkó DM, Thaler B, Szalay KZ, Fazekas D, Korcsmáros T, Csermely P. ComPPI: a cellular compartment-specific database for protein-protein interaction network analysis. Nucleic Acids Res. 2015;43(Database issue):D485–493.
31. The Gene Ontology Resource. 20 years and still GOing strong. Nucleic Acids Res. 2019;47(D1):D330–8.
32. Zhang B, Liu J, Li H, Huang B, Zhang B, Song B, Bao C, Liu Y, Wang Z. Integrated multi-omics identified the novel intratumor microbiome-derived subtypes and signature to predict the outcome, tumor microenvironment heterogeneity, and immunotherapy response for pancreatic cancer patients. Front Pharmacol. 2023;14:1244752.
33. Zhang B, Sun J, Guan H, Guo H, Huang B, Chen X, Chen F, Yuan Q. Integrated single-cell and bulk RNA sequencing revealed the molecular characteristics and prognostic roles of neutrophils in pancreatic cancer. Aging. 2023;15(18):9718–42.
34. Zhang S, Jiang C, Jiang L, Chen H, Huang J, Gao X, Xia Z, Tran LJ, Zhang J, Chi H, et al. Construction of a diagnostic model for hepatitis B-related hepatocellular carcinoma using machine learning and artificial neural networks and revealing the correlation by immunoassay. Tumour Virus Res. 2023;16:200271.
35. Yoshihara K, Shahmoradgoli M, Martínez E, Vegesna R, Kim H, Torres-Garcia W, Treviño V, Shen H, Laird PW, Levine DA, et al. Inferring tumour purity and stromal and immune cell admixture from expression data. Nat Commun. 2013;4:2612.
36. Li X, Guan H, Ma C, Dai Y, Su J, Chen X, Yuan Q, Wang J. Combination of bulk RNA sequencing and scRNA sequencing uncover the molecular characteristics of MAPK signaling in kidney renal clear cell carcinoma. Aging. 2024;16(2):1414–39.
37. Ru B, Wong CN, Tong Y, Zhong JY, Zhong SSW, Wu WC, Chu KC, Wong CY, Lau CY, Chen I, et al. TISIDB: an integrated repository portal for tumor-immune system interactions. Bioinf (Oxford England). 2019;35(20):4200–2.
38. Thorsson V, Gibbs DL, Brown SD, Wolf D, Bortone DS, Ou Yang TH, Porta-Pardo E, Gao GF, Plaisier CL, Eddy JA, et al. The Immune Landscape of Cancer. Immunity. 2018;48(4):812–e830814.
39. Zeng Z, Wong CJ, Yang L, Ouardaoui N, Li D, Zhang W, Gu S, Zhang Y, Liu Y, Wang X, et al. TISMO: syngeneic mouse tumor database to model

tumor immunity and immunotherapy response. Nucleic Acids Res. 2022;50(D1):D1391–7.
40. Zhang B, Yuan Q, Zhang B, Li S, Wang Z, Liu H, Meng F, Chen X, Shang D. Characterization of neuroendocrine regulation- and metabolism-associated molecular features and prognostic indicators with aid to clinical chemotherapy and immunotherapy of patients with pancreatic cancer. Front Endocrinol (Lausanne). 2022;13:1078424.
41. Gide TN, Quek C, Menzies AM, Tasker AT, Shang P, Holst J, Madore J, Lim SY, Velickovic R, Wongchenko M, et al. Distinct Immune cell populations define response to Anti-PD-1 monotherapy and Anti-PD-1/Anti-CTLA-4 combined Therapy. Cancer Cell. 2019;35(2):238–e255236.
42. Newman AM, Liu CL, Green MR, Gentles AJ, Feng W, Xu Y, Hoang CD, Diehn M, Alizadeh AA. Robust enumeration of cell subsets from tissue expression profiles. Nat Methods. 2015;12(5):453–7.
43. Finotello F, Mayer C, Plattner C, Laschober G, Rieder D, Hackl H, Krogsdam A, Loncova Z, Posch W, Wilflingseder D, et al. Molecular and pharmacological modulators of the tumor immune contexture revealed by deconvolution of RNA-seq data. Genome Med. 2019;11(1):34.
44. Tamminga M, Hiltermann TJN, Schuuring E, Timens W, Fehrmann RS, Groen HJ. Immune microenvironment composition in non-small cell lung cancer and its association with survival. Clin Translational Immunol. 2020;9(6):e1142.
45. Racle J, Gfeller D. EPIC: a Tool to Estimate the proportions of different cell types from bulk gene expression data. Methods Mol Biology (Clifton NJ). 2020;2120:233–48.
46. Aran D, Hu Z, Butte AJ. xCell: digitally portraying the tissue cellular heterogeneity landscape. Genome Biol. 2017;18(1):220.
47. Li T, Fan J, Wang B, Traugh N, Chen Q, Liu JS, Li B, Liu XS. TIMER: a web server for Comprehensive Analysis of Tumor-infiltrating Immune cells. Cancer Res. 2017;77(21):e108–10.
48. Jiang P, Gu S, Pan D, Fu J, Sahu A, Hu X, Li Z, Traugh N, Bu X, Li B, et al. Signatures of T cell dysfunction and exclusion predict cancer immunotherapy response. Nat Med. 2018;24(10):1550–8.
49. Becht E, Giraldo NA, Lacroix L, Buttard B, Elarouci N, Petitprez F, Selves J, Laurent-Puig P, Sautès-Fridman C, Fridman WH, et al. Erratum to: estimating the population abundance of tissue-infiltrating immune and stromal cell populations using gene expression. Genome Biol. 2016;17(1):249.
50. Sun D, Wang J, Han Y, Dong X, Ge J, Zheng R, Shi X, Wang B, Li Z, Ren P, et al. TISCH: a comprehensive web resource enabling interactive single-cell transcriptome visualization of tumor microenvironment. Nucleic Acids Res. 2021;49(D1):D1420–30.
51. Yuan H, Yan M, Zhang G, Liu W, Deng C, Liao G, Xu L, Luo T, Yan H, Long Z, et al. CancerSEA: a cancer single-cell state atlas. Nucleic Acids Res. 2019;47(D1):D900–8.
52. Yang C, Zhang H, Chen M, Wang S, Qian R, Zhang L, Huang X, Wang J, Liu Z, Qin W et al. A survey of optimal strategy for signature-based drug repositioning and an application to liver cancer. eLife 2022, 11.
53. Morris GM, Huey R, Lindstrom W, Sanner MF, Belew RK, Goodsell DS, Olson AJ. AutoDock4 and AutoDockTools4: automated docking with selective receptor flexibility. J Comput Chem. 2009;30(16):2785–91.
54. Trott O, Olson AJ. AutoDock Vina: improving the speed and accuracy of docking with a new scoring function, efficient optimization, and multithreading. J Comput Chem. 2010;31(2):455–61.
55. Van Der Spoel D, Lindahl E, Hess B, Groenhof G, Mark AE, Berendsen HJ. GROMACS: fast, flexible, and free. J Comput Chem. 2005;26(16):1701–18.
56. Abraham MJ, Murtola T, Schulz R, Páll S, Smith JC, Hess B, Lindahl E. GROMACS: high performance molecular simulations through multi-level parallelism from laptops to supercomputers. SoftwareX. 2015;1–2:19–25. Medium: X; Size: p.
57. Huang R, Zhou PK. DNA damage repair: historical perspectives, mechanistic pathways and clinical translation for targeted cancer therapy. Signal Transduct Target Therapy. 2021;6(1):254.
58. Germano G, Amirouchene-Angelozzi N, Rospo G, Bardelli A. The clinical impact of the genomic Landscape of Mismatch Repair-deficient cancers. Cancer Discov. 2018;8(12):1518–28.
59. Moynahan ME, Jasin M. Mitotic homologous recombination maintains genomic stability and suppresses tumorigenesis. Nat Rev Mol Cell Biol. 2010;11(3):196–207.
60. Heitmeir B, Deniz M, Janni W, Rack B, Schochter F, Wiesmüller L. Circulating Tumor cells in breast Cancer patients: a Balancing Act between Stemness, EMT features and DNA damage responses. Cancers 2022, 14(4).
61. Ushijima T, Clark SJ, Tan P. Mapping genomic and epigenomic evolution in cancer ecosystems. Sci (New York NY). 2021;373(6562):1474–9.
62. Papanicolau-Sengos A, Aldape K. DNA methylation profiling: an emerging paradigm for Cancer diagnosis. Annu Rev Pathol. 2022;17:295–321.
63. Xiong J, Chi H, Yang G, Zhao S, Zhang J, Tran LJ, Xia Z, Yang F, Tian G. Revolutionizing anti-tumor therapy: unleashing the potential of B cell-derived exosomes. Front Immunol. 2023;14:1188760.
64. Ivashkiv LB. IFNγ: signalling, epigenetics and roles in immunity, metabolism, disease and cancer immunotherapy. Nat Rev Immunol. 2018;18(9):545–58.
65. Jardim DL, Goodman A, de Melo Gagliato D, Kurzrock R. The challenges of Tumor Mutational Burden as an Immunotherapy Biomarker. Cancer Cell. 2021;39(2):154–73.
66. Samstein RM, Lee CH, Shoushtari AN, Hellmann MD, Shen R, Janjigian YY, Barron DA, Zehir A, Jordan EJ, Omuro A, et al. Tumor mutational load predicts survival after immunotherapy across multiple cancer types. Nat Genet. 2019;51(2):202–6.
67. Li K, Luo H, Huang L, Luo H, Zhu X. Microsatellite instability: a review of what the oncologist should know. Cancer Cell Int. 2020;20:16.
68. Sadeghi S, Quinn D, Dorff T, Pal S, Groshen S, Tsao-Wei D, Parikh R, Devitt M, Parikh M, Jackovich A, et al. EphrinB2 inhibition and Pembrolizumab in Metastatic Urothelial Carcinoma. J Clin Oncology: Official J Am Soc Clin Oncol. 2023;41(3):640–50.

Publisher's note